Metrol. Meas. Syst., Vol. 29 (2022) No. 3, pp. 429–454
DOI: 10.24425/mms.2022.142273

PAN POLSKA AKADEMIA NAUK

METROLOGY AND MEASUREMENT SYSTEMS

Index 330930, ISSN 0860-8229
www.metrology.wat.edu.pl

M&MS

ANATOMICAL AND FUNCTIONAL ASSESSMENT OF PATENCY OF THE UPPER RESPIRATORY TRACT IN SELECTED RESPIRATORY DISORDERS – Part 2

Andrzej Zając[1)], Andrzej Kukwa[2)], Robert Barański[3)], Szymon Nitkiewicz[4,5)], Edyta Zomkowska[6,7)], Adam Rybak[8)]

1) *Military University of Technology, Warsaw, Institute of Optoelectronics, Kaliskiego St., 2, 00-908, Warsaw, Poland* (*andrzej.zajac@wat.edu.pl*)
2) *University of Warmia and Mazury, Olsztyn, Department and Clinic of Otorhinolaryngology, Head and Neck Diseases, Collegium Medicum, Warszawska St. 30, 10-082 Olsztyn, Poland* (*andrzejkukwa41@gmail.com*)
3) *AGH University of Science and Technology in Kraków, Department of Mechanics and Vibroacoustics, Mickiewicza St. 30, 30-059 Kraków, Poland* (*robertb@agh.edu.pl*)
4) *University of Warmia and Mazury in Olsztyn, Department of Mechatronics, Faculty of Technical Science, Oczapowskiego St. 2, Olsztyn, Poland* (*szymon.nitkiewicz@gmail.com*)
5) *University of Warmia and Mazury in Olsztyn, Department of Neurosurgery, School of Medicine, Oczapowskiego St. 2, Olsztyn, Poland*
6) *Clinic of Otorhinolaryngology, Head and Neck Surgery, University Hospital in Olsztyn, Warszawska St. 30, 10-082 Olsztyn, Poland*
7) *University of Warmia and Mazury,in Olsztyn, Department and Clinic of Otorhinolaryngology, Head and Neck Diseases, Collegium Medicum, Warszawska St. 30, 10-082 Olsztyn, Poland*
8) *LABSOFT Sp. z o.o., Puławska St. 469, 02-844 Warsaw, Poland* (✉ *adam.rybak3@gmail.pl*, +48 501 651 802)

Abstract

This article presents selected physical diagnostic methods used in otorhinolaryngology and results of their application. In addition to the applications of methods using the capabilities of selective sensors, selected methods of hybrid diagnostics were also presented – for assessment of parameters of respiratory processes, with polysomnography as an example of using both typical diagnostic methods dedicated to otolaryngology, as well as standard EEG and ECG methods. It has been shown that in some special cases of respiratory disorders, measurements of the air flow in the respiratory tract can be supplemented with pressure measurements in selected positions within the airways. The presented optical methods and diagnostic systems are very often used in the diagnosis of diseases not specific for otolaryngology occurring in the area of the head and neck. The presented material is the second part of the study discussing both standard and widely used diagnostic methods. All presented methods are dedicated to otolaryngology. This text is a continuation of the material published in No 4 of 2021 [1].

Keywords: optical diagnostic in otolaryngology, upper respiratory tract diagnostics, otolaryngology, spirometer, Fourier transform, wavelet transform, quantitative parameters of the respiratory cycle.

Article history: received March 16, 2022; revised June 11, 2022; accepted June 26, 2022; available online July 28, 2022.

1. Introduction

Rapidly developing measurement techniques and emerging new physical methods are frequently used in otolaryngological diagnostics. A wide range of applied diagnostic methods constitute the basis for the review study aimed at presenting selected modern diagnostic methods and presenting diagnostic results to a wider group of users. In this part, the methods based on measuring the respiratory parameters of patients were analysed. Respiration is the most important and necessary action to support life and its effective duration. It is an actual gas exchange in the respiratory system consisting of removing CO_2 and supplying O_2. Gas exchange occurs in the alveoli, and an efficient respiratory tract allows for effective ventilation. A disruption in the work of the respiratory system leads to measurable disturbances in blood saturation and consequently, hypoxia. Frequent, even short-term, recurrent hypoxia in any part of the body leads to multiple complications. This is largely related to theduration of hypoxia as well as the processes that accompany it. The causes of hypoxia resulting from impaired patency of the respiratory tract and/or the absence of neuronal respiratory drive can be divided into the following groups depending on the cause: peripheral, central and/or of mixed origin. Causes of the peripheral form of these disorders are largely due to the impaired patency of the upper and/or lower respiratory tract. Therefore, an early diagnosis and location of these disorders can be prevent complications. Slow, gradually increasing obstruction of the *upper respiratory tract* (URT) is not noticeable and becomes a slow killer. Hypoxic individuals in a large percentage of cases have a shorter life expectancy and, above all, deal with the consequences of hypoxia much sooner.

2. Selected methods for hybrid diagnosis of essential parameters of respiratory processes

2.1. Pressure distribution diagnostics in the upper airway region

In certain specific cases of respiratory disorders, the airflow measurements in the respiratory canals can be complemented by pressure measurements at a selected point of the respiratory tract. The measuring system, a diagram of pressure distribution diagnostics in the upper airway region, and examples of results are shown in Fig. 1. The pressure waveforms obtained at individual measuring points enable the correlation of its variability with the physiological and anatomical changes being searched for in the upper airway region. If the flow parameters in the respiratory canals, measured by other methods (partial pressure of the inhaled and exhaled air, which can be determined at the same time in a parallel measurement, after adding the determined physiological parameters in the patient's circulatory system, *e.g.* changes in blood saturation) are used, a comprehensive diagnosis of the respiratory system condition can be obtained.

The graphics provided in Fig. 1 on the right show, in sequence, the profiles obtained during the pressure measurement:

- the pressure waveform in the nasal respiratory canals (#1) – a slow change in the pressure value, with a low variability amplitude is measured, which is obvious when we consider the fact that the measurement site is directly linked to the environment through the open nasal canals,
- another measuring point (#2): the oral cavity – here, pressure fluctuations that represent the natural respiratory cycle that is manifested by changes in the alternating cycles of positive and negative pressure are more pronounced than those in the nasal canal – the recorded changes are correlated in time with smaller fluctuations in the waveform recorded in the nasal canal,

Metrol. Meas. Syst., Vol. 29 (2022), No. 3, pp. 429–454
DOI: 10.24425/mms.2022.142273

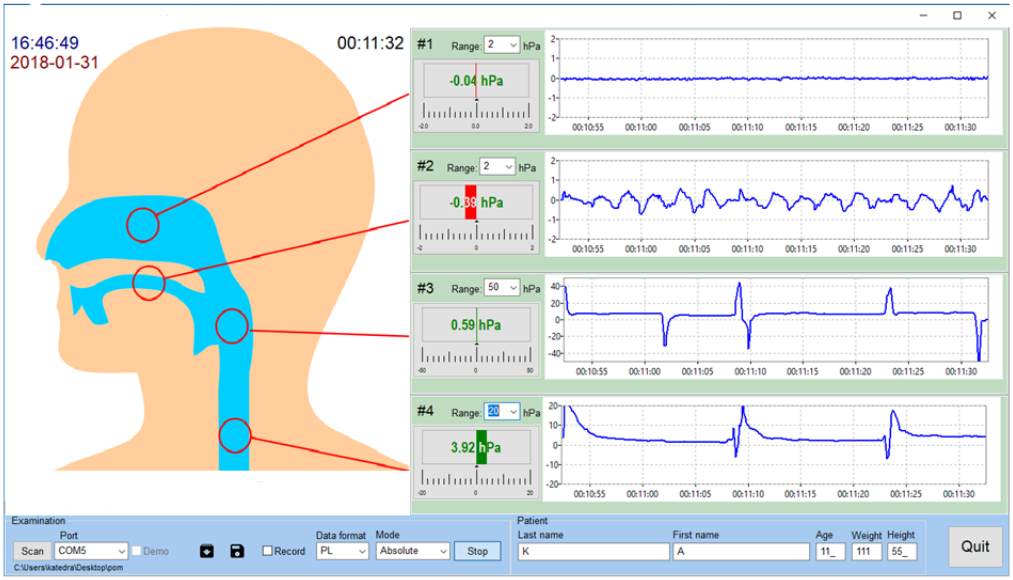

Fig. 1. A diagram of the measuring system (on the left, the pressure measurement points in the oral cavity, nasal cavity, and trachea are indicated by red circles), and (on the right) examples of pressure measurement results at the indicated points of the respiratory tract. In the figure, the measurement site (red circle) was graphically assigned to the obtained graph.

– the pressure waveform in the glottal region (#3) is shown in the next diagram – the change in the pressure amplitude is due to swallowing saliva,
– another pressure diagram (#4) – a waveform of pressure changes in the oesophagus – enables the diagnosis of possible disorders related to the gastroesophageal reflux disease.

2.2. Polysomnographic examination

A highly developed version of the examination, which enables recording of both the respiratory activity and many associated physiological parameters, is the polysomnographic examination. This examination is mainly used to record changing parameters of the human body during sleep. Depending on the anticipated sleep disorders, different sensors are used, and various parameters are recorded. An example of test stand instrumentation (Fig. 2) and the examination results (Fig. 2) are shown in subsequent figures. A polysomnographic examination involves the following four basic techniques:

– electroencephalography (EEG) – electrodes are placed on the patient's head to assess the bioelectric activity of the brain
– electrocardiography (ECG) – electrodes are placed on the patient's chest to assess the electrical activity of the heart
– electrooculography (EOG) – electrodes are placed near the patient's eyes to investigate changes in the action currents generated during the movements of the eyeball and after exposure to light flashes
– electromyography (EMG) – electrodes are placed on the patient's body to assess muscle and nerve function.

Fig. 2. A view of a patient equipped with sensors during a polysomnographic measurement.

The measuring system shown in Fig. 2 was configured with a unit for flow measurement in three respiratory canals – the method of operation and examples of the results of the use of NasoOroSpirometer were discussed in previous sections of the presented study. The use of the above-mentioned unit allows additional information to be obtained on both the airway patency and the quantitative flows in each respiratory canal, including the abnormalities found. In addition, a microphone, a temperature sensor, and (an) airflow sensor(s) are placed in the mouth region. A limb movement sensor is placed on the patient's ankle, and a pulse oximeter is placed on a finger, and the so-called 'respiratory belts', which record the movements of these body parts, are placed on the abdomen and chest. In addition, a body position sensor is required as well. In complex systems, it can be converted into a separate recording and analysis of the video recorded in a measurement session. Both the sensors and the electrodes are installed in such a manner so as not to excessively restrict the examined patient's movements. If the patient needs to go to the toilet at night, it will not be problematic, as it is sufficient to disconnect the electrodes from the apparatus.

A camera is usually located in a corner of the room in which the examination is being performed. It is used for the overnight recording of the patient's motor responses during sleep. Besides the camera, an additional body position sensor is often installed at a selected point of the patient's body, which enables the recording of the body's position during sleep without the need for further detailed analysis of the video recording. It is also possible to install an actimeter, $i.e.$ a limb movement sensor that is most commonly placed on the ankle. All of the data are sent to the computer. A person trained in sleep medicine sits in an adjacent room all night to monitor the course of the examination and, if necessary, correct the position of electrodes in case they are displaced during the examination.

As compared to the diagnostic unit presented in Fig. 2, coupled with the developed (Part 1 [1]) NasoOroSpirometer – a typical unit comprises only one sensor that monitors the airflow during breathing – a diagram described on the printout as AIRFLOW – indicating the respiratory rhythm but not allowing to obtain (without performing a calibration procedure individually for each patient) the quantitative measurements related to the examined patient's breathing (Fig. 3). In order to compare the results of flow measurements during gas exchange, obtained using

Metrol. Meas. Syst., Vol. 29 (2022), No. 3, pp. 429–454
DOI: 10.24425/mms.2022.142273

the NasoOroSpirometer and original polysomnographic instrumentation in relation to respiratory parameters, it is worth comparing the examples of results obtained from both apparatuses (Fig. 3). Thus, the advantage of the developed device enables the following:

- the behaviour of the function of airflow in individual respiratory canals over time is recorded, with the possibility to select the recording system configuration – each nasal canal independently – both inspiration and expiration – inspiration and expiration through the mouth and any combination of both cases mentioned,
- during the examination, it is possible to record each flow independently, which enables not only the qualitative assessment of the asymmetry of flows but also their quantitative assessment,
- the recording of the waveform enables the provision of quantitative values of the inspiration and expiration volume, and with these values being specified for each canal, a possibility for performing a spirometric examination,
- despite the differences in the flow measurement using a thermo-anemometer sensor, related to the varying humidity of the inhaled and exhaled air, the calculation of the inhaled and exhaled air volumes, both in a single respiratory cycle and in cycles of selected duration, is possible and not affected by significant errors.

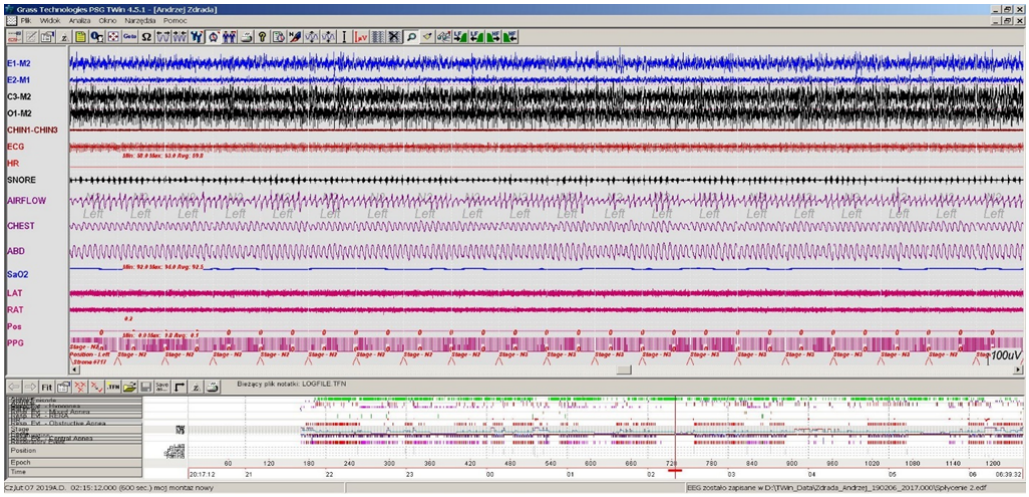

Fig. 3. An exemplary screenshot showing a recorded set of waveforms with the variability of parameters that are important during an polysomnographic examination. Sequentially from the top: E1-M2 – electrooculogram (E1 – right eye, M2 – reference electrode), E2-M1 – electrooculogram (E2 – left eye, M1 - reference electrode), C3-M2 and O1-M2 – EEG (C3 and O1 – electroencephalography and electrodes on the head, M2 – reference electrode, CHIN1-CHIN3 – tension from the submental muscles, electrodes, ECG – electrocardiogram, ECG, HR – heart rate, SNORE – snoring sounds, AIRFLOW – air flows through the nose and mouth (or only through the nose), pressure sensor, CHEST – respiratory movements of the chest, ABD – respiratory movements of the abdomen, SaO_2 – blood saturation, LAT and RAT – lower limb movements, e.g. accelerometer sensor, Pos – body position, PPG – photoplethysmogram.

The metrological parameters of the sensors used to measure the amount of air flow in individual URT (*upper respiratory tract*) channels are presented in Part 1 of the article [1]. In the case of polysomnographic tests, the number of measured parameters – both the physiological parameters of the patient (ECG, EEG, heart rate, blood oxygenation), as well as the necessary physical quantities (position of the limbs, the patient's body system), the number of parameters measured, the range of their variability measured during the test are determined by the set of sensors used by the manufacturer.

The results obtained during the polysomnographic examination are currently the standard for diagnosing sleep disorders, for example presented in Fig. 4. However, in many cases, detailed diagnostics of only the respiratory cycle during sleep is sufficient to detect sleep apnoea, and, in many cases, it allows an initial diagnosis to be given.

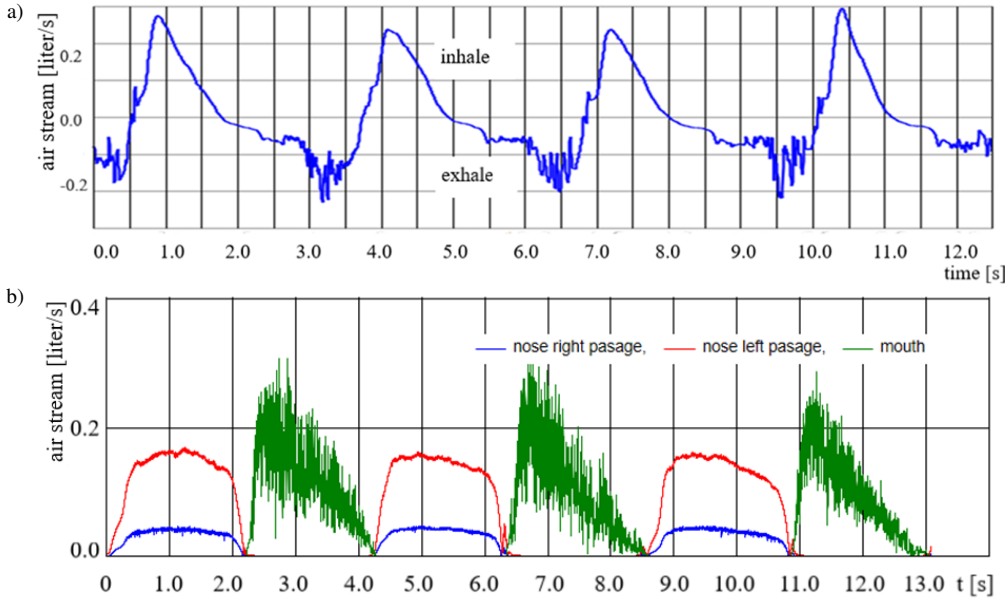

Fig. 4. Examples of the results of flow measurement using a sensor for recording respiratory activities recorded during a polysomnographic examination. Because of the sensor used, this is a qualitative waveform (left nasal canal), and for the calibration for the purpose of quantitative measurements, an additional calibration procedure would be required each time (for each individual patient) (a), and the results of measurement obtained using the NasoOroSpirometer developed by the authors – the quantitative measurements for all respiratory canals were recorded (b). The bottom figure shows a clear, approximately three-fold difference in the volume of the flow through the nasal canals, both right and left, resulting from improper nasal structure due to anatomical abnormalities.

All of the measurement data (in medicine: diagnostic information) obtained using metrological systems enable the improvement of quality and promptness of patient diagnostic procedures with regard to respiratory system parameters.

3. Diagnostic imaging

Simple optical diagnostic methods and systems are very often involved in the diagnostics of diseases occurring in the head and neck region, except for neurological issues. The simplest method, which has been traditionally known and used is a visual inspection that enables typical disease symptoms to be recognised. Doctors use this method at the initial stage of diagnosing the patient (it is also used as a standard in diagnoses made by general practitioners) and use specialised optical systems, *e.g.* specialised ENT endoscope systems. Rapid diagnostics using X-rays can also be part of diagnosing more complex cases. Such diagnosis is possible in real-time due to the technical possibility for digital recording of X-ray photographs and, in recent times, it has also been possible for *spiral computed tomography* (SCT) due to its low emission of radiation.

Metrol. Meas. Syst., Vol. 29 (2022), No. 3, pp. 429–454
DOI: 10.24425/mms.2022.142273

3.1. X-ray

An examination using the Müller's manoeuvre can be an example of application of diagnostic imaging in the spectral X-ray range . During this manoeuvre, the patient attempts to inhale with the mouth closed and the nostrils shut, which, due to the forced negative pressure in the upper airway region, results in the collapse of the airway lumen. There are diagnostic apparatuses which allow measurement data to be obtained in two versions. Moreover, fluoroscopy or computed tomography (in particular SCT due to the promptness of the examination) can be used. An example of results obtained using SCT is presented in Fig. 5. Two time points of such an examination are shown in Figs. 5a and 5b, respectively. The extent of changes in the lumen of the respiratory canals, provided that there is a physiological basis for this, *e.g.* soft palate relaxation, can provide the basis for diagnosing the causes of sleep apnoea, including disorders associated with loud snoring. This technique is designed to find disorders in the upper airway, *e.g.* the trachea. Diagnostics using Müller's manoeuvre is used, *inter alia*, to precisely determine the physiological causes of sleep apnoea. The representative example of the results obtained from SCT tomographic examination (presented in Fig. 5) shows a possible cause of sleep apnoea, *i.e.* an ongoing soft palate problem. In addition to the qualitative assessment of the examination results (Fig. 5), a detailed quantitative analysis is also possible.

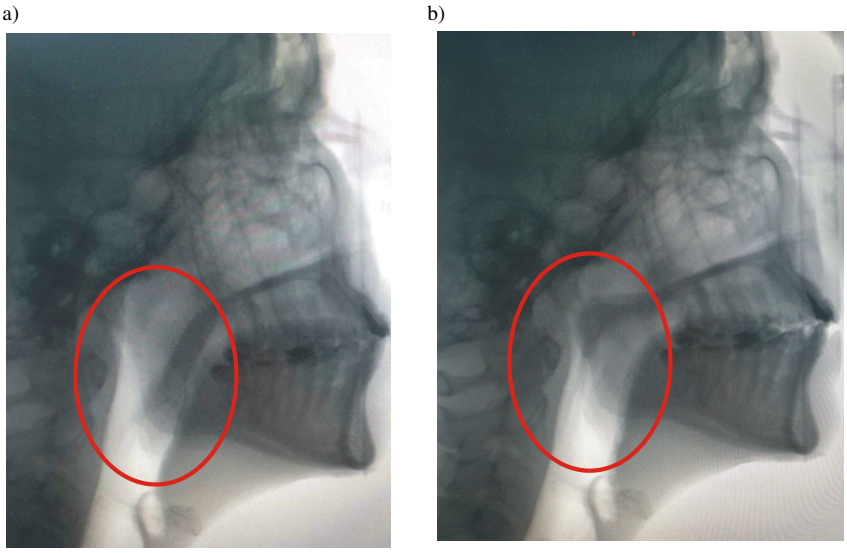

Fig. 5. The anatomical ratio in the area of the lower pharynx as well as the soft palate and uvula were visualised during the Müller's manoeuvre: resting position (a), dynamic position (b). The red curve marks the area of quantitative measurements of the volume of respiratory canals in the URT.

An outline of the analytical procedure developed by the authors of the study for the case above is presented below. Considering that, in the diagnostic method discussed, the area under observation is considerably smaller than the entire CT image, the imaging area is intentionally limited. At the same time, due to the known characteristics of the area under examination, the dynamic range of the grey levels is reduced from the typical 256 levels to 60 levels. Consequently, the results of analysis of the studied image take the form presented in Fig. 5, for selected analytical procedures listed in the following figures. The figure shows the essential steps of the analytical procedure being prepared.

The reasons why the diagnostics using the Müller's manoeuvre in the present form are not commonly applied include the potential hazard of ionising radiation (X-ray examination with the option of digital image recording using silicone matrices, including the fluoroscopic technique with the option of video recording during the examination), and the high costs of examination with CT methods. Figs. 5 and 6 show the effect of using a *spiral CT* (SCT) system in an examination. In view of the costs of both the equipment and the examination, the methods for dynamic imaging of internal structures using fluoroscopy are competitive to SCT imaging-based methods.

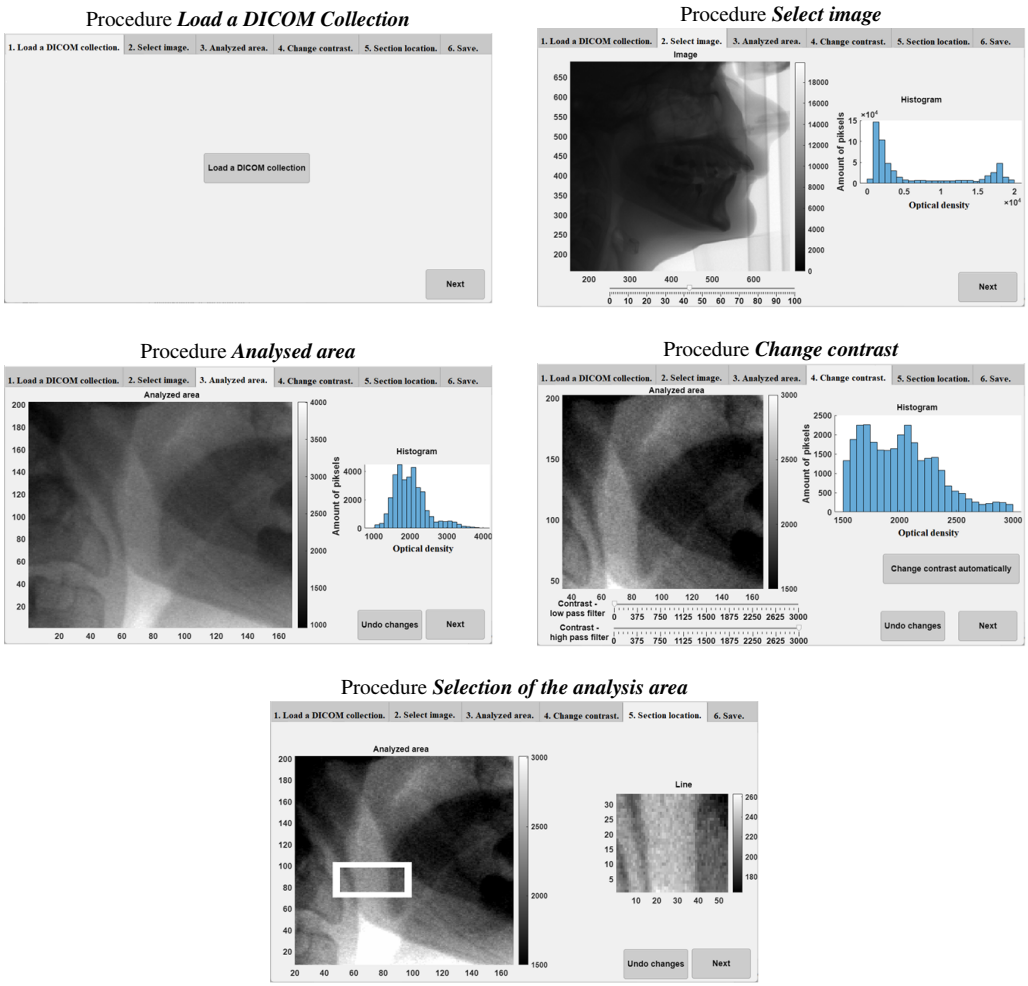

Fig. 6. Selected stages of the Müller's manoeuvre analysis using the developed numerical procedure that enables an analysis of the upper airway region image. The figures indicate the names and effects of the modules.

3.2. Endoscopic

In addition to the medical diagnostic imaging carried out in the X-ray spectral range, devices operating in the VIS spectral range have become increasingly common since the development of different types of optical endoscopes and fiberscopes. The widespread use of such equipment, in

particular, using optical fibre cables (flexible endoscopes), represents a broad area of application in the field of diagnostics, including examinations performed via natural body orifices. This method is complemented by the methods of visualisation of the areas being operated through incisions made in the skin to initiate a surgical procedure, integrally related to laparoscopic surgical techniques. Recently, the importance of fibre optic cables has decreased due to the availability of CMOS cameras with at least a VGA standard (for VGA, the matrix dimensions are 480×640 pixels, up to 1920×1080 pixels seen in chips, all that for the size of up to 5.5 mm). Under such an arrangement, the image from the CCD (or CMOS) matrix surface is sent in an electrical form to the visualisation system, *i.e.* a monitor, usually an LCD, but there are also simple endoscopic systems with the option of visualisation on a phone display. The concept of both systems still used in flexible endoscopes is presented in Fig. 7.

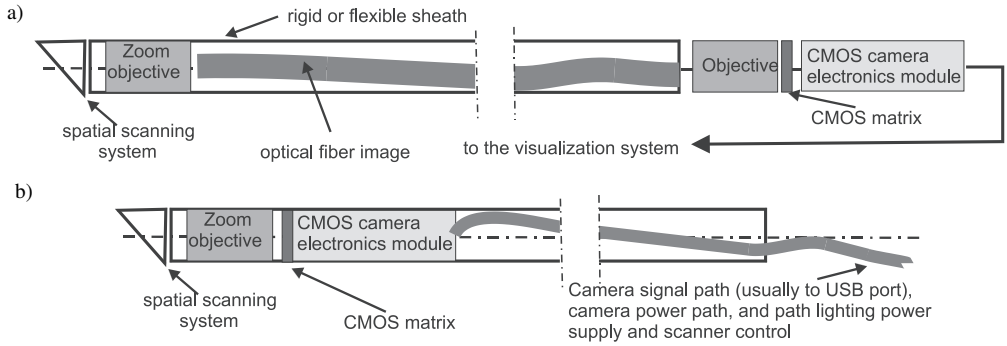

Fig. 7. Typical solutions of endoscopic imaging systems: a) fiberscope, b) videoscope (each of them can be either a rigid or flexible system).

Each examination using optical methods, including endoscopic ones, requires good quality imaging to be effective, as it is necessary to obtain the best possible image of the observed area. In both endoscopic imaging methods being discussed, the limitations on obtaining a good quality image are different. When using a system with a miniature CMOS camera, the resolution of the obtained image is determined by the standard of the chip in the camera used, while the use of a fiberscope results in the limitation caused by the geometry of the optical fibre bundle and the fiberscope front face diameter, *e.g.* the diameter of the fiberscope front face $\Phi = 2.1$ mm (active surface of the fibre system is 1.5 mm), the diameter of a single fibre is 11 μm, and the number of fibres is 16,000 [29]. Two fundamental facts are worth noting here:

- the VGA image visualisation standard (one of the lower ones used in this imaging technique) is over 300 000 pixels,
- the lifetime of the fibre optic line (resulting from fibre degradation due to the defects arising during the line bending that is natural during the examination) is considerably lower than the lifetime of a chip, estimated at 20 years, which is a period longer than the technical acceptance period for the camera.

In specialised laryngological treatment, simple diagnostics based on optical methods are being extended to include endoscopic examinations and imaging examinations in the X-radiation range, including computed tomography that enables 3D imaging of the area under examination. As regards oncology diagnostics, 3D imaging is also supplemented by the *magnetic resonance imaging* (MRI) technique.

In typical optical diagnostic procedures carried out in the VIS range, it is possible to determine the condition of the mucous membrane of the nasal, oral, and pharyngeal cavity, and, based on

the assessment of the monitored surface, allows a diagnosis to be made for typical lesions found on it, *i.e.* inflammation, local damage (Fig. 8) to the mucous membrane, disruptions in the geometry of the diagnosed canals and surfaces, and the location of possible polyps. A similar inspection range is followed to determine the condition of the ear canal for the lesions typical of this organ. Novel studies in the field of optical diagnosis techniques are also appearing (the possibility for determining the parameters of distortion and deformation of the organs under observation, and for performing absolute measurements of surface parameters and the 3D shape of the biological structures under observation), as well as proposals of hybrid measuring systems which significantly increase the precision of the measurements performed. The applied methods and procedures for the diagnosis of otorhinolaryngological disorders include, within their scope, diagnostics of anatomical areas with considerable parameters of variability in terms of both time and space. More specifically, certain areas subject to diagnostics produce oscillating motion, others change their hydration, changes occur in both the gas flow parameters in the respiratory canals and in the geometrical parameters of the respiratory passages. Another area subject to diagnostics are the organs of hearing, including the glottal region and the internal ear. One of the areas subject to frequent examination is the eardrum which vibrates when exposed to acoustic stimuli.

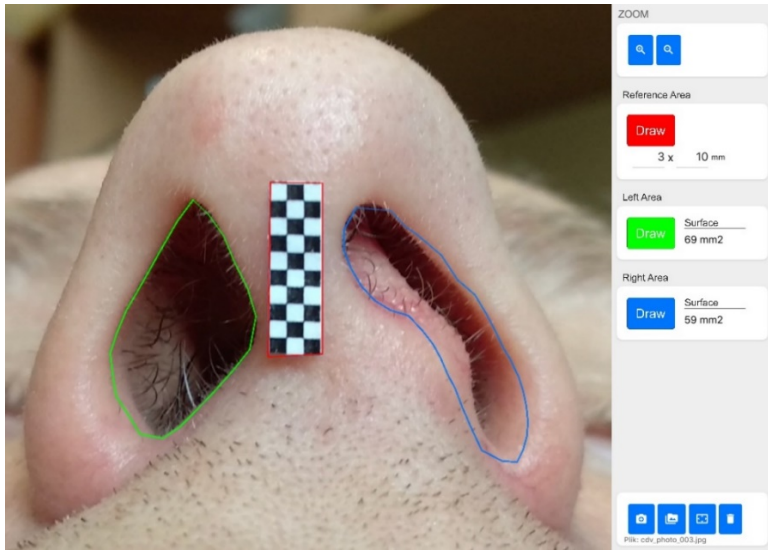

Fig. 8. An example of graphical analysis of asymmetry of nasal canals: the difference between the cross-section of the left nasal canal (green) and that of the right nasal canal (grey) is clearly visible. The chequered pattern applied when taking photographs enables the determination of absolute quantities obtained from the measurements. The colours applied to the openings of the nasal canals result from the operation performed by the authors of the system for the purposes of graphical analysis – the program interface is shown in the figure.

3.3. 3D imaging in CT and 2D in VIS spectrum

Diagnosing the eardrum often involves its response to acoustic stimulation and an examination of electrical signals in the nervous system. The examination often involves the patient listening to specific sounds (tones, acoustic frequencies) and producing a response for the operator when the patient can hear them. This examination only provides information on the defect and its size, yet it

provides no information on the site of the defect emergence for the purposes of further treatment. For this reason, new methods are being sought to enable an easy assessment of the site of damage and to allow the process of diagnosing the patient to be shortened.

The discussion of diagnostic methods related to imaging, *i.e.* visualisation and analysis of the obtained image, can begin with the simplest methods, *e.g.* photographic imaging. An example of diagnostic use of photography and graphical image analysis methods is presented in Fig. 9. The developed image analysis procedure enables a quantitative assessment of the cross-sectional area of the respiratory nasal canals, which allows, *e.g.* the quantitative flow measurement results to be compared, allowing for a conclusion about other limitations in the respiratory canals.

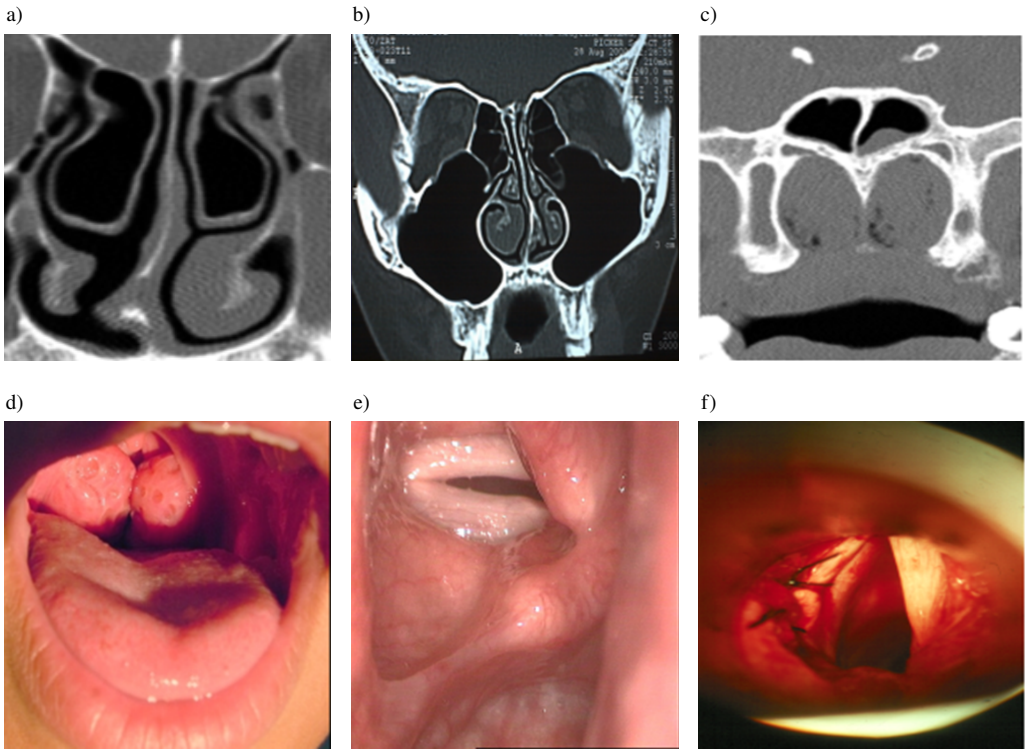

Fig. 9. Selected examples of the use of tissue imaging the upper row provides examples of results obtained in a CT examination, while the lower one shows visible light imaging. The successive figures show: a) crooked nasal septum on the right, a protruding spike narrows the inferior nasal passages, small inferior nasal concha. On both sides, enlarged middle conchas – aerated areas significantly obturate the nasal passages. On the left – compensatory hypertrophy of the inferior concha, b) the so-called narrow nose: hypertrophy of the inferior nasal conchas causes the obstruction of both nasal cavities, c) visible blockade of the posterior nostrils by the total pharyngeal tonsil mass, d) visible much enlarged palatine tonsils, the so-called kissing tonsils, e) paralysis of both vocal cords, f) abduction of the vocal cords following paralysis – abduction sutures are visible.

Figure 9 shows cases of combined photographic imaging (2D) and spatial tomographic imaging (3D). A jointly performed graphical analysis of both the photographs (the bottom row in Fig. 9) and the selected tomogram projections (the top row in Fig. 9) enables to diagnose the asymmetry in the size of the nasal canals as significant (as that in Fig. 9 on the left), anatomic asymmetries found in the glottal region (Fig. 9, in the middle). In all images shown in Fig. 9,

smaller or larger asymmetry is noticeable in the respiratory system – the difference in the cross-sectional area of the respiratory canal can significantly affect the patient's breathing parameters.

The presented selected possibilities of diagnostic imaging, both the most complex, as CT and MRI, and the simpler optical methods (both technically and analytically, in terms of the measurement result processing) concern the field of otorhinolaryngology, *i.e.* a field of medicine that specialises in diagnosing and treatment of diseases in the head and neck region. Otorhinolaryngology became a separate field of medicine in the early 20th century through combining certain domains of otology and laryngology.

The optical methods, allow us, in addition to the basic functions of 2D imaging, to obtain information about the depths. Usually, we can only perform visual observation of the examined object's surface, *e.g.* as shown in Fig. 9, however, it is also possible to get information about depths, when using complex measurement procedures, *e.g.* OCT, to obtain information on the interior of the examined organ. Simpler optical methods used in novel endoscopic solutions also enable representation of the 3D structure of the examined area using stereoscopy or the speckle analysis method.

3.4. Stereoscopic endoscope set

The analysis of diagnostic possibilities for these areas will begin with endoscopic techniques using 3D imaging. Endoscopic observation is characterised by an imperfection related to the problem of estimating the actual size of the object being recorded, for both an exact and estimated measurement. This problem is tackled in different ways. As regards universal endoscopes without built-in measuring procedures, an experienced operator is able to estimate the dimension of the object being recorded based on the knowledge of the characteristics of the observed objects or, more precisely, of their surroundings. The operator estimates the object's dimension using the points or reference lines (*e.g.* veins) being observed. For endoscopes with the camera positioned at an angle of 90 degrees in relation to the direction of endoscope insertion, *i.e.* for example, for borescopes, it is possible to roughly estimate the size of the observed object through rotation. On the other hand, for fiberscopes or videoscopes, the measurement uncertainty when performing such a measurement is much higher [2, 36, 37]. The problem of measurement accuracy in fiberscopes or videoscopes is solved with attachments with a measuring grid installed on the eyepiece. These attachments have measuring grids of various shapes, *e.g.* cross, cylindrical, or angular. Unfortunately, a limitation on the use of attachments is the need to determine the distance between the lens and the surface being examined. The solution is to design a system for sharp observation of the object only at a specified distance between the object and the lens. When the object is observed from a different distance, its image is blurred. The next generation of endoscopes uses image analysis methods that enable the use of different probes equipped with, *e.g.* double-camera systems of "*stereo measurement*", or a camera and projector system of "*shadow measurement*". Another method uses laser radiation to scan surfaces [2, 3].

The most important functionalities of a stereovision system include not only the dimensioning of components within the imaging area but also 3D visualisation. Fig. 10 shows a diagram of a stereoscopic endoscope, while Fig. 11 shows a simplified algorithm for 3D image generation. In addition, it is possible to apply an algorithm responsible for dimensioning objects.

Several algorithms are known to support the dimensioning of objects and to be able to produce a 3D image using a set of colour or polarisation filters. Choosing the right algorithm is crucial and determines the accuracy of the method. The most promising algorithm is the one for matching blocks separated according to preset parameters in both 2D photographs (Block Matching), which is characterised by the smallest error in maintaining the linearity of the objects being dimensioned.

Metrol. Meas. Syst., Vol. 29 (2022), No. 3, pp. 429–454
DOI: 10.24425/mms.2022.142273

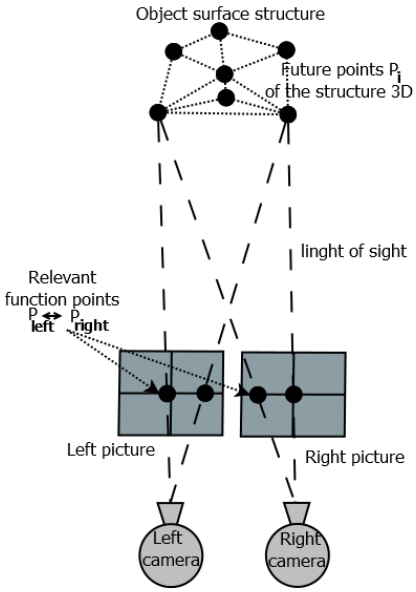

Fig. 10. A diagram of a selected stereoscopic object imaging system.

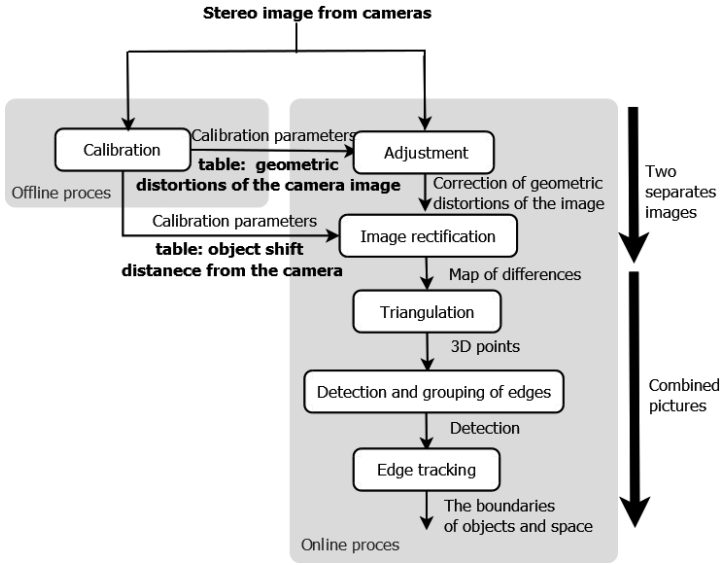

Fig. 11. Algorithm for image processing in a stereoscopic testing device.

In addition to the possibility for plotting (preparing) a drawing that uses the representation that gives an impression of a 3D visualisation from two recorded 2D images obtained with stereoscopic imaging it is also possible to use this technique in film recording. The existing solutions used in diagnostics and therapy support are usually based on the use of colour filters assigned to each of the observer's eyes.

The use of 3D imaging technologies in typical diagnostic techniques is currently beginning to fill the existing niche in ENT diagnostics [5].

Issues of this type are particularly relevant to the area of endoscopic diagnostics. This occurs for two particular reasons:

– The dimensions of an endoscope and the requirements for the design of stereoscopic devices necessitate very high precision for such designs.
– Obtaining 3D imaging, in a version from both a stereoscopic system and devices that enable numerical reconstruction of geometry of the examined surface using structured light [16] is a process that changes doctors' habits.

3.5. Endoscopic methods for voice cord diagnostics

An example of imaging that enables the macro-scale use of stereophotographs to visualise complex tissue structures is shown in Figure 12. the circuit to be miniaturised. The systems that enable the acquisition and reproduction of spatial information on an object, *i.e.* 3D visualisation, allow the operator to observe the changes over time which is determined by the fact that the projection of images onto the observer's retina with a frequency significantly above 25 Hz is perceived as continuous information. Hence the attempt to obtain the so-called time magnifier which enables the visualisation of rapidly changing processes occurring within the human body.

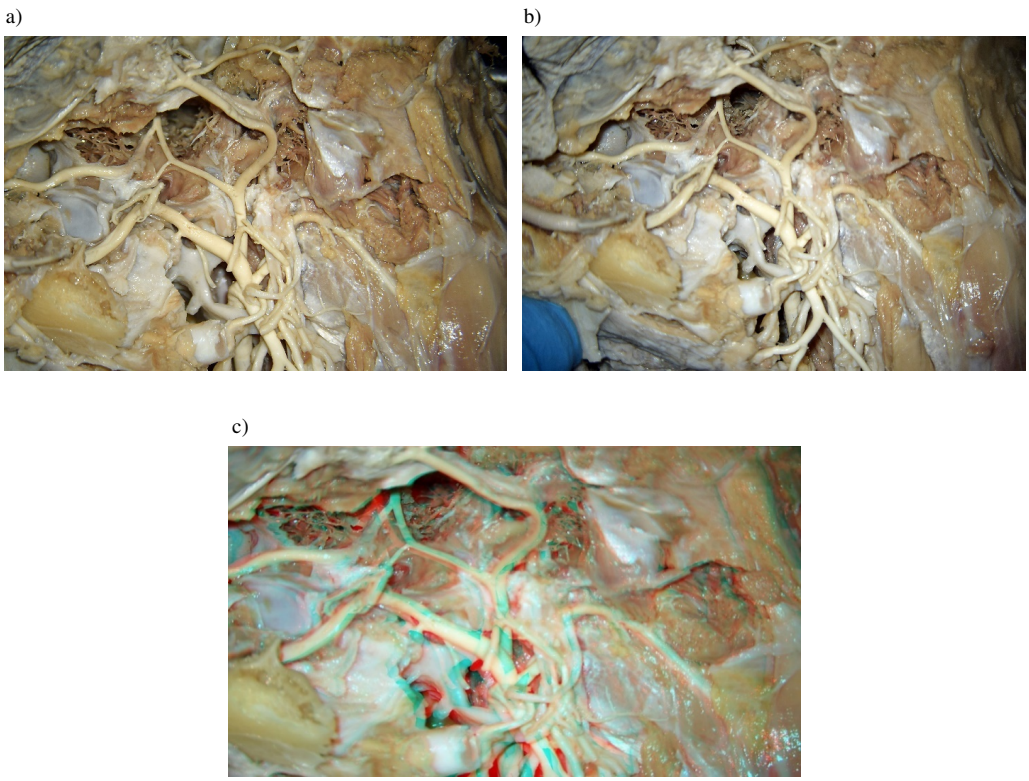

Fig. 12. An example of use of stereophotographs: a) a photograph from the left lens, b) a photograph from the right lens, c) an anaglyph – a combination of 2D photographs into an arrangement that enables 3D observation using two-colour glasses.

Metrol. Meas. Syst., Vol. 29 (2022), No. 3, pp. 429–454
DOI: 10.24425/mms.2022.142273

The current state-of-the-art as regards the technique of recording fast-changing waveforms allows the recorded image to be saved and later reproduced at a lower speed. The available cameras enable this procedure with a frequency of image recording from 4K quality (4 096 × 2 304 pixels) for the recording rate of 938 frames per second to the resolution, obtained in miniature models, of 1 280 × 1 024 pixels with a frequency ranging from 915 frames per second to as many as 52 445 frames per second for the 128 × 8 matrix. The use of this technique for recording fast-changing processes, but mainly for analysing the obtained enormous datasets, is not always justified. A stroboscope, which has been used since its invention in the 1830 s, enables a simple visualisation of the vibrations of the vocal cords and (possibly) the eardrum, in real-time, provided that we are able to both excite a specific type of vibration of the examined organ and illuminate, with a preset frequency, the area under observation with a series of short pulses of light with relatively high luminance. Previous solutions were based on the use of a discharge lamp, which required a relatively powerful power supply system operating at a voltage level ranging from several hundred volts to kVs. It is currently possible to apply systems with LEDs, which enables the development of a stroboscopic circuit with a power supply operating at a voltage of several volts, thus allowing the circuit to be miniaturised.

3.6. Endoscopic methods with structured light

The literature provides many proposed solutions that enable visualisation of selected characteristics of the organ being examined in the the upper airway region using optical methods [30–35]. For the visualisation of fast-changing processes occurring in the human body, structured light methods can be employed as well [26, 27]. A brief summary of applicable structured light techniques is provided in Fig. 13.

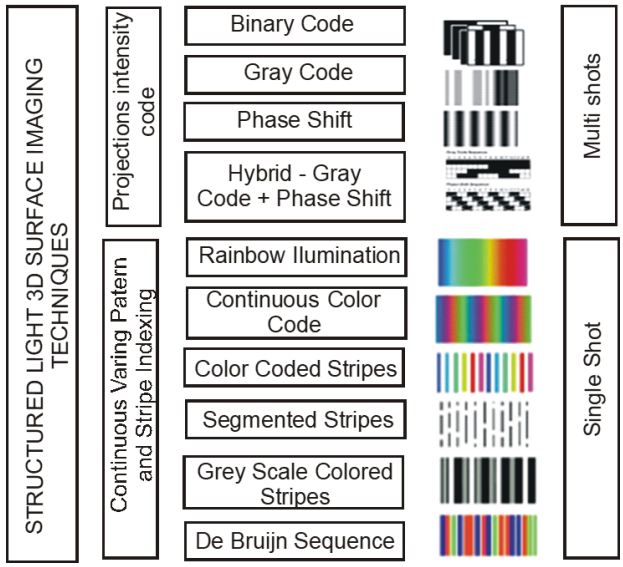

Fig. 13. A compilation of selected methods for analysing the surface shape using structured light. The selected methods include both those requiring the analysis of multiple exposures at different spatial and temporal parameters of the illumination of the examined surface and those using complex coding methods but allowing a result from a single exposure with structured light to be obtained – based on [18].

The techniques using structured light enable high-speed scanning of structures with varying shapes, including when fulfilling appropriate geometrical conditions, also 3D objects within the entire space. It is usually required to take multiple scans for different directions of the code projection and then to merge the obtained images of parts of the examined object. The rate of obtaining 3D imaging is very attractive when generating digital 3D models of humans. The diagnostics of large areas of the patient's surface are usually used in orthopaedics, yet this can also be successfully applied for smaller organs, in which case the main problem is to determine the abnormal deviations of the examined object, *e.g.* dentition or anomalies within the glottal or auricular region. 3D structured light scanners are lightweight devices that enable the precise selection of representation accuracy through selection of structured light parameters. They are, however, very sensitive to lighting conditions, as any shadows cast on the object are represented in the generated 3D file. However, this defect is not of particular significance in medical examinations due to typical shapes of examined objects.

The authors proposed a system enabling the visualisation of eardrum vibrations using a modified ENT endoscope – Fig. 14. The next Fig. 15 shows a proposed system for the endoscopic examination of the eardrum using the illumination of the eardrum surface with flat figures formed using the LED light.

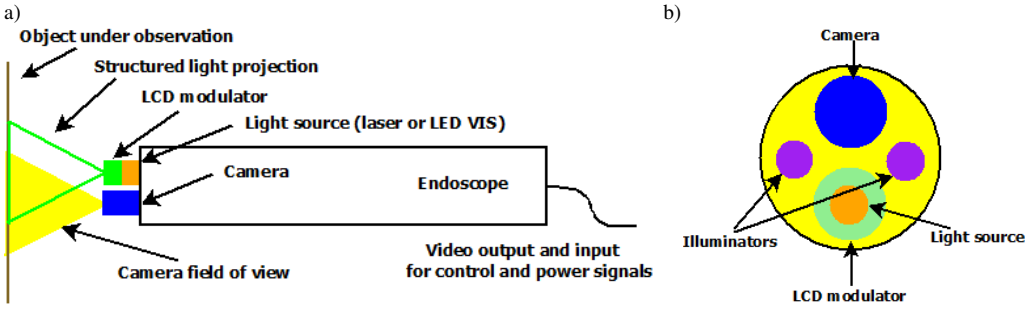

Fig. 14. An example of the proposed solution of a rigid endoscope system for examination of eardrum dynamics: a) diagram of the system (the eyepiece is not shown – a typical design approach), b) a view of the endoscope front.

The proposed endoscopic system comprises several essential components:

- An illuminating system constructed from LED emitters – an RGB emitter matrix with a power of up to 100 mW each (two matrices), which enables the application of the method for adjusting the colour temperature of the illuminating source [17, 19].
- A miniature 2 mm camera produced according to the VGA standard.
- A structured light emitter – due to the dimensions of the endoscope transducer, the classical design using Gray codes [18] was replaced, after analysis of the examination's specificity, with an LCD matrix that allows selected closed lines to be obtained – Fig. 12. The entire emitter additionally contains a semiconductor laser (or a monochromatic LED) that emits radiation in the VIS range.

Examples of imaging of effects of such an examination, *i.e.* the determination of the eardrum dynamics through an analysis of changes in the geometry of illumination, are shown for selected cases of eardrum vibration modes in Fig. 16. The examination allows for the visualisation and (after the recording and analysis of the recorded illumination distributions) the quantitative parameters of the eardrum deviations from the equilibrium position. The proposed solution, which involves the projection of one or several selected monochromatic lines, is much simpler in contrast to the classical method for projecting bands selected according to the Gray

Metrol. Meas. Syst., Vol. 29 (2022), No. 3, pp. 429–454
DOI: 10.24425/mms.2022.142273

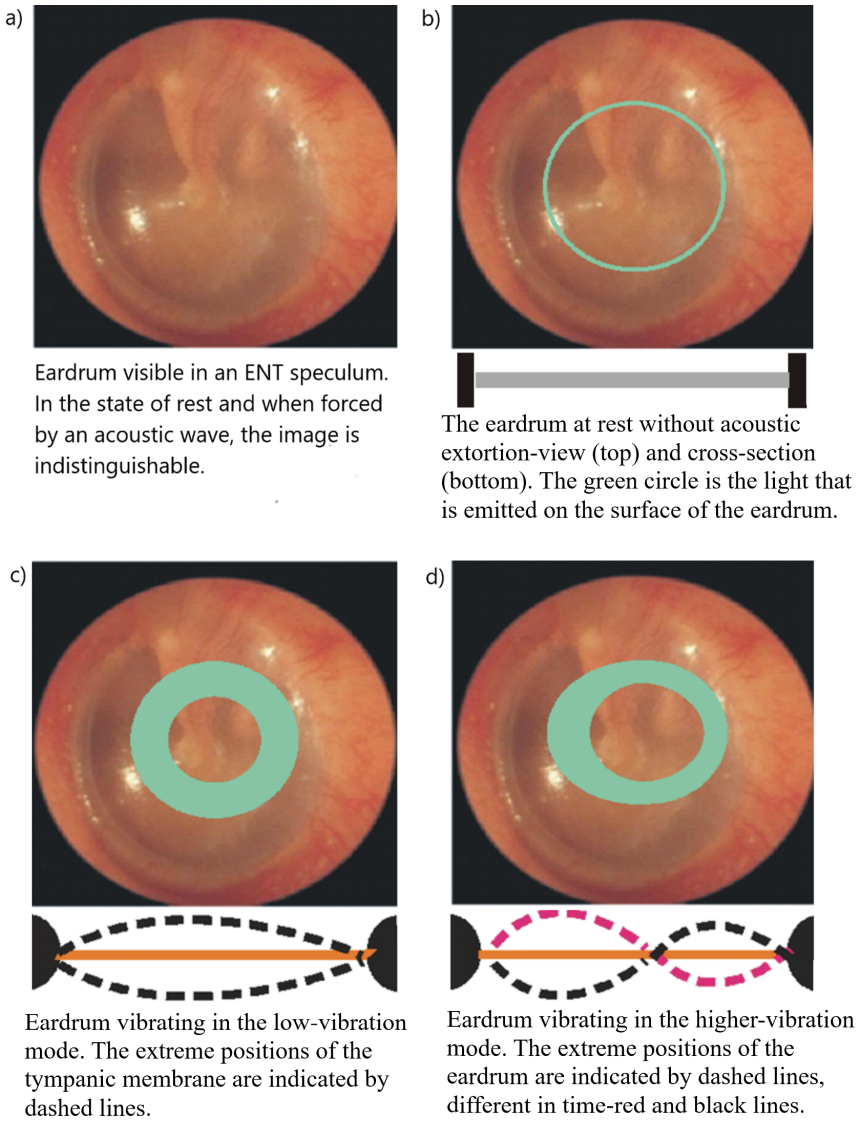

Fig. 15. A change in the geometry of the coloured shape being emitted (green line) on the surface at rest (b), and after a change in the geometry of the examined eardrum (in medical diagnostics, these can be eardrum vibrations), caused by the excitation with an acoustic wave with a frequency similar to the resonant frequency for low-vibration modes (resonant frequencies of the eardrum vibrations) – (c) and d). The green line on the eardrum surface corresponds to the vibration mode defined by the black dotted line. Figure a) indicates the view in a classical ENT speculum – the absence of a displayed line. Eardrum defects will be manifested by deformations of the reference line.

code, and thus much quicker to analyse. It can therefore be equally effective as well, particularly when we have additional knowledge of physical characteristics of the examined object and, as regards the analysis of eardrum dynamics, we have such knowledge (and an accurate mathematical model). This methodology is also applicable in diagnosing the condition of the glottis [35].

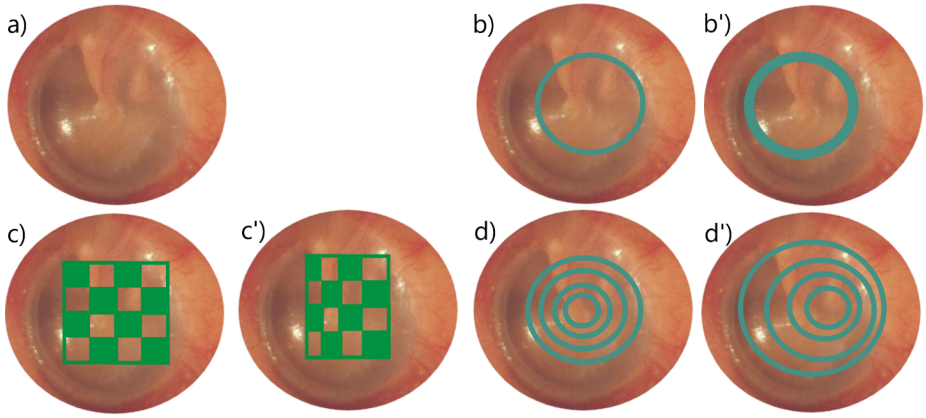

Fig. 16. Examples of the structured light structures dedicated to analysis of eardrum movement; a) an endoscopic image of the eardrum at rest, b) and b') a circle displayed on the eardrum surface, which enables the analysis of the eardrum deflection amplitude during acoustic excitation with a low-frequency tone, c) and c') – a structure designed to analyse the verification of the position of the axis of the endoscope's optical system in relation to the eardrum surface. In the further part of the examination, the analysis of the light geometry deformation on the eardrum surface allows for a conclusion about the condition of surface vibrations, d) and d') a structure designed to analyse amplitude distribution during acoustic excitation, based on spherical geometry. Figures b), c) and d) show the initial condition, while b'), c') and d') show the post-deformation condition.

4. Interferometry in otorhinolaryngological diagnostics

The interferometric methods, those using classical interferometers and, more commonly, the speckle [20] and holographic [19] methods, are characterised by the highest measurement resolution; therefore, it is possible to represent the deformations of the examined object with a resolution of the order of the wavelength of the radiation source being used. Let us consider briefly the methods referred to.

Speckle photography is a non-contact optical measurement method using correlation between the incident beam and the scattered beam from the surface of the object being measured. It enables the measurement of object displacements in the direction parallel to the object's surface, the measurement of displacements in the direction of the incident beam, the angle of normal rotation to the surface of the examined object, and the performance of levelling of the examined object [19, 20, 36]. In this method, coherent laser radiation (usually VIS, but very often He-Ne laser radiation) is used to illuminate the surfaces of the object being examined.

Adjacent fragments of the coherent laser radiation beam interfere with one another, thus creating a structure of fine dark (subtraction of electric field vectors) and bright (addition of electric field vectors) speckles distributed within the beam's space – Fig. 17.

The classical procedure for measuring the deformations of a surface that exhibits Lambertian reflectance by the speckle method involves taking two photographs (when the required energy relations are maintained, it is not important whether these are classical or digital photographs): the first one before the object deformation, and the second one, on the same photogram, after the deformation. After taking the double photograph and developing it (superimposing the digital exposure and the matrix raster), an object is obtained which causes the scattering of radiation, *i.e.* the deflection of the reproducing radiation beam on the diaphragm borders represented as a result of the recording of speckle distributions. Each recorded distribution results in a separate

Metrol. Meas. Syst., Vol. 29 (2022), No. 3, pp. 429–454
DOI: 10.24425/mms.2022.142273

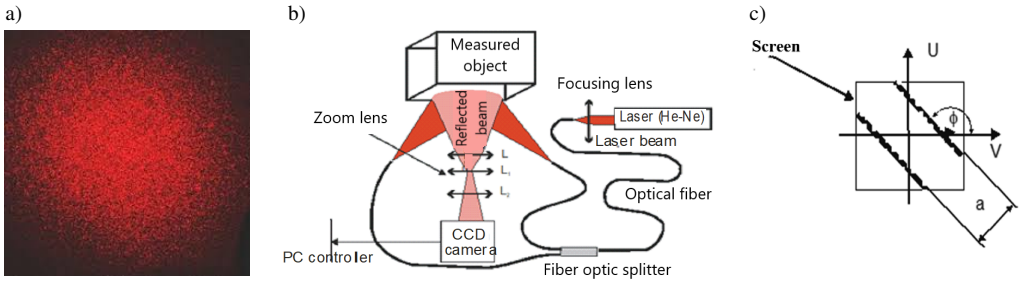

Fig. 17. A diagram for discussing the speckle method. The successive figures show: a) the effect of He-Ne laser beam self-interference, b) a diagram of the measuring system using CCD camera recording for measurements, c) the diagram shows the relationships used in the deformation analysis by the method concerned.

arrangement of diffraction wave (wavefront) distributions corresponding to a particular speckle family. Consequently, a two-dimensional analogue of Young's experiment is obtained (for the case of monochromatic light illumination). The speckle method has a significant limitation on the accuracy of deformation analysis (as compared to classical interferometric methods) – it enables the determination of displacements of the studied surface within the range of changes of its position from tenths of a millimetre [28].

The value of surface displacement, possible to determine using speckle methods, is considerably higher than those possible to obtain with interferometric methods, where the achieved measurement sensitivity amounts to as much as 1/200 of the radiation wavelength, which for the He-Ne laser is just over 3 nm. As regards the digital photography-based method, there are no problems with the analysis of fast-changing objects. It appears that the only limitation is the speed of photographic recording, which results in conditions for the illumination systems used.

Holography – in order to conclude the considerations as regards the measurement possibilities of both topography and changes in the geometry of the examined object in space and time, a brief discussion on the most precise optical diagnostic method is necessary. The interferometric methods, including holographic ones (in particular, double-pulsed holography), enable the determination of the distribution of deformations of the object under study with an accuracy of an order of a fraction of the wavelength of the laser used in the measuring system. What is particularly worth mentioning are the requirements necessary in performing the diagnostics of biological centres with this method. In classical holography (a diagram of the measurement stand is provided in Fig. 18), spatial distribution of the interference field obtained from the effect of both the reference beam, which is not subject to changes in the recording process and the beam concerned, disturbed by the object, is recorded on a light-sensitive material (holographic plate subjected to chemical treatment, photorefractive or photothermal materials). By recording the distribution of the band field, we obtain information on both intensity (light wave electrical field amplitude) and change in the amplitude of the wave concerned in relation to the reference wave.

In this way, complete information on the radiation reflected from the test object (which is being recorded) is obtained. A requirement necessary for recording a hologram, *i.e.* complete information about the radiation beam reflected from the object under study, is to maintain the unchanged condition of the object (with an accuracy of up to 1/8 of the wavelength applied) during the recording. The time required for the recording of a hologram is primarily determined by the accuracy of the material tooling (*i.e.*, how many details there are) used and the energy contained in the laser beam.

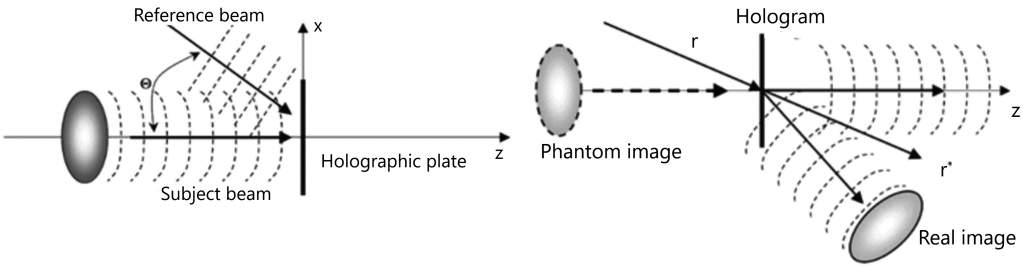

Fig. 18. A diagram of a laboratory system for hologram recording (on the left) and a system for hologram reading (on the right). For the recording on a light-sensitive material, two coherent beams are required – one source and division of the beam in such a manner that the beam reflected from the object and the reference beam have a similar intensity (as no division into two equal parts is involved!). In the system for beam reconstruction, in order to maintain the geometry of object representation, it is required to use a beam with the same wavelength and geometry of the reference beam as during the recording.

It is only possible to fulfil this condition for living objects by using pulsed lasers [20, 22]. Hence, in the diagnostics of time-varying biological objects, double-pulsed holography is used – two states of the distribution of the concerned beam phase, stretched over time, are recorded – two consecutive exposures with the selected separation time. Attempts are known to have been made to use double-pulsed holography in medicine. It suffices to recall the papers presented as early as the 1980s by Pluta in [20], which contain analysis of the glottis vibration field carried out using a pulsed ruby laser radiation (Cr^{3+}:Al_2O_3). More extensive work on the medical applications of interferences using optical fibres, *i.e.* work in the endoscopic area, was performed by Podbielska's team [21]. An example of reproduction of a double-pulsed hologram created at the Institute of Optoelectronics, Military University of Technology, is presented in Fig. 19.

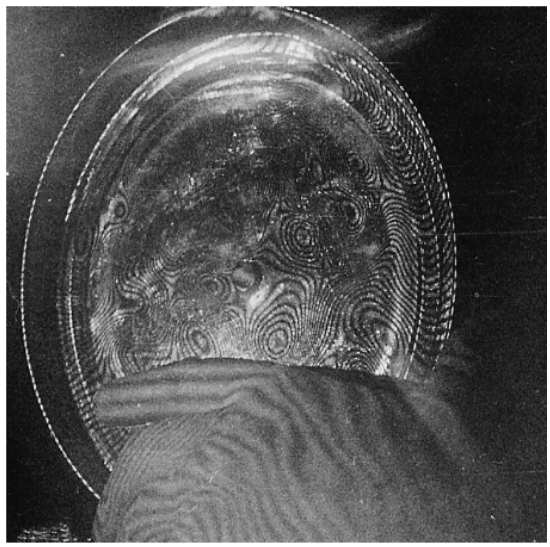

Fig. 19. A reconstructed interferogram of a hand-held membrane, created using a holocamera system with a double-pulsed ruby laser. For medical applications, the distributions of the band field are of interest – in the photograph, these are the bands on the hand holding the membrane [24].

Classical interferometric systems – the interference field is recorded in these applications on a selected surface of the object under examination – are applied to analyse interference field distribution using detection systems. Holocameras are used to record biological objects and if the goal to be achieved is to record – and later on, to reproduce the object's 3D holographic image – the band field generated is a result of the effect of the beam concerned and the reference beam, It should be noted that at the current stage of medical applications, they are used in few cases due to the high cost, $e.g.$ to analyse the distribution of the patient's surface vibrations. Meanwhile, many studies concern the application of fibre optic interferometers. The main difference between both of these systems concerns the method for recording the obtained interferograms – field methods are used in classical interferometry, $i.e.$ the interferogram is recorded at a specific moment in time for the entire surface being examined (an example of a field interferogram is the photograph shown in Fig. 14). As regards optical fibre interferometers, instantaneous radiation intensity over a certain time interval is recorded – thus, the information on the period and distribution of the banding distribution amplitudes for the interfering reference beam and the beam concerned is obtained. Therefore, two different pieces of information are obtained: spatial banding distribution for a selected moment in time (classical interferometry) or a change at a selected point in space for a selected time interval (optical fibre interferometry) – $e.g.$ [25]).

5. The use of virtual reality technology

There are several commonly known and applied techniques for producing stereoscopic photographs, $i.e.$ creating the illusion of three-dimensionality of the observed scene. This approach has a history dating back to 1853, when Wilhelm Rollann [6] came up with his invention. Currently, three methods for displaying 3-dimensional images are used [7]: stereograms [8, 9], layer-stacking methods [10], and wavefront reconstruction methods based on Gabor's concept [11]. The 3D representation method using stereophotography techniques, which have been in use for several decades, requires the use of two-colour glasses or glasses with polarising filters to observe the compiled 3D image. The version involving two-colour glasses results in a change in the colours of the scenes being observed.

The current development of VR-related electronic methods allows this shortcoming to be eliminated. The combination of real-time 3D imaging (two flat images recorded in 4K resolution) with a frame rate corresponding to that of a film (over 25 frames per second) allows this technology to be applied in training sessions for medical personnel. In order to make the training of doctors more realistic, it is also necessary to transfer, to the Virtual Reality area, instruments, e.g. microsurgical ones, which are also virtual but represented through controllers associated with the trainees' hands, and which transfer the movements of hands holding virtual instruments into the virtual operative field. The IT technologies currently in place enable such operations. As an example, scientists from the University of Washington have developed a surgery simulator to provide training in the patient's skin suturing technique on a virtual training model [12]. A simulator for nasal endoscopic procedures also operates based on the above-mentioned technique and provides the opportunity to learn how to perform therapeutical interventions on a virtual plane and diagnose lesions in a simulated region [13, 14].

The great advantage of using both virtual and augmented reality is the number of simultaneous participants of such a training course. When the training participants are looking through the microscope binocular (operator) or through an auxiliary viewing eyepiece (assistants, members of the trainee team) only two, and sometimes three, of them can observe the operator's actions simultaneously while maintaining all the parameters related to viewing the operative

field. When using VR, all the members of the trainee team participate in an exemplary surgical procedure. There are many advantages of virtual medical education delivered in this manner. Not only do they include an atlas of anatomical structures dedicated to the area of training issues, but also offer the opportunity to virtually simulate actual surgical procedures while ensuring very high compatibility between the virtual and physical reality. As regards training in acquiring or consolidating, *e.g.* surgical habits, it is possible to combine (simultaneous action on combined spaces, *i.e.* the virtual and the imaging of the actual space) scenes for the training being provided. An unlimited number of trials and repetitions can be selected for such a training session. A training course participant does not feel the pressure of the other group members who could otherwise force too fast (or too slow) a pace of work, and he/she can repeat the trained sequences many times. Training sessions using *virtual reality* (VR) are already commercially available, including training for medical professionals, *e.g.* a training session entitled *The Induction of a New Paramedic*, where, thanks to pre-prepared ambulance simulation, a job candidate can, in a safe environment, learn about all the components an ambulance is equipped with [15, 38–40].

6. Summary

The presented article (this text is a continuation of the material published in No 4 of 2021 [1]) discusses selected physical diagnostic methods applicable in otorhinolaryngology. The diagnostic procedures and methods (mainly optical) discussed in detail were selected in consideration of the existing development possibilities of the presented solutions. Each of the methods presented in the paper has its advantages and disadvantages, makes use of different physical phenomena, and enables the observation of specific characteristics of the lesions under study. In order to make a correct diagnosis quickly and precisely, it is required to perform an examination using a variety of methods. When selecting the presented solutions, it was also taken into account that in many indicated procedures it is possible, in the current state of technology, to significantly increase the diagnostic accuracy as many components of the procedure being performed using developed and dedicated measurement methods considerably increase the speed and precision of analysis. The presented methods allow different diagnostic methods to be combined, which increases the volume of measurement data to be analysed but allows hidden correlations to be found which may not be apparent in each individual method. One such opportunity is the investigation of events at the intersection of different medical specialties, with a current example being the diagnosing of sleep apnoea.

The authors, while presenting selected diagnostic methods, have also tried to present the results of their own studies conducted in this field of research, as well as the designs developed for their implementation, taking into account the possibility for the hybridisation of the developed solutions in order to expand the diagnostic possibilities and improve their accuracy and precision. This trend in the development of diagnostic instrumentation is one of the leading solutions, including the automation of diagnostics using artificial intelligence. Efforts are also underway to ensure that certain methods are interchangeable and others complementary. Undoubtedly, the applied methods constitute an area allowing for improvement of precision of medical diagnostics in the field of otorhinolaryngology. The solutions proposed can be supplemented with new possibilities, both qualitative and quantitative. Considering that the individual methods are different and offer various diagnostic possibilities, it appears to be crucial to develop solutions that enable their combination.

References

[1] Kukwa, A., Zając, A., Barański, R., Nitkiewicz, S., Kukwa, W., Zomkowska E., & Rybak, A. (2021). Anatomical and functional assessment of patency of the upper respiratory tract in selected respiratory disorders – Part 1. *Metrology and Measurement Systems*, *28*(4), 813–836. https://doi.org/10.24425/mms.2021.138538

[2] Stöppler, M. C. (2018). CT Scan (CAT Scan, Computerized Tomography) Imaging Procedure. *MedicineNet*. https://www.medicinenet.com/cat_scan/article.htm

[3] Nałęcz, M., Torbicz, W., Zawick, I., Chmielewski, L., Kulikowski, J., Nowakowski, A., Cudny, W., Kozińska, D., & Chmielewski, L. (2003). Biocybernetyka i Inżynieria Biomedyczna 2000 Tom 8 – Obrazowanie Medyczne. Akademicka Oficyna. *Wydawnicza EXIT*, Warsaw.

[4] Wachulak, P. W., Marconi, M. C., Bartels, R. A., Menoni, C. S., & Rocca, J. J. (2008). Soft x-ray laser holography with wavelength resolution. *JOSA B*, *25*(11), 1811–1814. https://doi.org/10.1364/JOSAB.25.001811

[5] Mahmood, F., Chen, R., & Durr, N. J. (2018). Unsupervised reverse domain adaptation for synthetic medical images via adversarial training. *IEEE Transactions on Medical Imaging*, *37*(12), 2572–2581. https://doi.org/10.1109/TMI.2018.2842767

[6] Rollmann, W. (1853). Zwei neue stereoskopische Methoden. *Annalen der Physik*, *166*(9), 186-187. https://doi.org/10.1002/andp.18531660914 (in German)

[7] Rojas, G. M., Gálvez, M., Vega Potler, N., Craddock, R. C., Margulies, D. S., Castellanos, F. X., & Milham, M. P. (2014). Stereoscopic three-dimensional visualization applied to multimodal brain images: clinical applications and a functional connectivity atlas. *Frontiers in Neuroscience*, *8*, 328. https://doi.org/10.3389/fnins.2014.00328

[8] Zone, R. (2014). Stereoscopic cinema and the origins of 3-D film, 1838-1952. *University Press of Kentucky*.

[9] Wheatstone, C. (1842). Beiträge zur physiologie des gesichtssinnes. *Annalen der Physik*, *131*(S1), 1–48. https://doi.org/10.1002/andp.18421310102 (in German)

[10] Rawson, E. G. (1969). Vibrating varifocal mirrors for 3-D imaging. *IEEE Spectrum*, *6*(9), 37-43. https://doi.org/10.1109/MSPEC.1969.5213672

[11] Berkley, J., Turkiyyah, G., Berg, D., Ganter, M., & Weghorst, S. (2004). Real-time finite element modeling for surgery simulation: An application to virtual suturing. *IEEE Transactions on visualization and computer graphics*, *10*(3), 314–325. https://doi.org/10.1109/TVCG.2004.1272730

[12] Gabor, D. (1948). A New Microscopic Principle. *Nature*, *161*, 777–778. https://doi.org/10.1038/161777a0

[13] Kim, Y., Park, J. S., & Kim, S. W. (2019). Virtual reality simulators for endoscopic sinus and skull base surgery: the present and future. *Clinical and Experimental Otorhinolaryngology*, *12*(1), 12–17. https://doi.org/10.21053%2Fceo.2018.00906

[14] Won, T.-B., Hwang, P., Lim, J.H., Cho, S.-W., Paek, S.H., Losorelli, S., Vaisbuch, Y., Chan, S., Salisbury, K., Blevins, N. H. (2018). (2018, January). Early experience with a patient-specific virtual surgical simulation for rehearsal of endoscopic skull-base surgery. *In International Forum of Allergy & Rhinology* (Vol. 8, No. 1, pp. 54–63). https://doi.org/10.1002/alr.22037

[15] Kwasniewski, K. (2021, June 5). *Przykłady wykorzystania VR 360 w szkoleniach e-learningowych*. eTechnologie. https://etechnologie.pl/vr-360-w-szkoleniach-e-learningowych (in Polish)

[16] Pirga, M., Kozłowska, A., & Kujawińska, M. (1993). Generalization of the scaling problem for the automatic moiré and fringe projection shape measurement systems. *Physical Research*, *Academic Verlag*, 188–193

[17] Gryko, Ł., Zając, A., Błaszczak, U. (2019). Characterization of multi-emitter tunable led source for endoscopic applications. *Metrology and Measurement Systems*, *26*(1), 153–169. https://doi.org/10.24425/mms.2019.126332

[18] Weisstein, E. W. (2008). Gray code. *From MathWorld – A Wolfram Web Resource*. https://mathworld.wolfram.com/GrayCode.html

[19] Gryko, Ł., & Zając, A., (2015). The use of LEDs in medicine, In *Problemy metrologii elektronicznej i fotonicznej*. In J. Mroczka (Eds.), *Problemy metrologii elektronicznej i fotonicznej* (pp. 123–171). Oficyna Wydawnicza Politechniki Wrocławskiej (in Polish)

[20] Pluta, M. (Ed.). (1984). *Holografia optyczna*. PWN. (in Polish)

[21] Kaufmann, G. H. (Ed.). (2011). *Advances in speckle metrology and related techniques*. John Wiley & Sons. https://doi.org/10.1002/9783527633852

[22] Kreis, T. (2006). *Handbook of holographic interferometry: optical and digital methods*. John Wiley & Sons. https://doi.org/10.1002/3527604154.indauth

[23] Podbielska, H. (1991, August). Trends in holographic endoscopy. In Holography, Interferometry, and Optical Pattern Recognition in Biomedicine (Vol. 1429, pp. 207–213). SPIE. https://doi.org/10.1117/12.44668

[24] Bobak, W., Borowicz, L., Jankiewicz, Z., & Kęcik, T. (1978). Badania nad możliwością wykorzystania holografii świetlnej w diagnostyce jaskry. *Klinika Oczna*, *48*(80), 647–650 (in Polish)

[25] Kondrat, M., Szustakowski, M., Gorka, A., Palka, N., Zyczkowski, M., & Niznik, S. (2004, November). Modal interference fiber optic sensor. *In Unmanned/Unattended Sensors and Sensor Networks* (Vol. 5611, pp. 225–232). SPIE. https://doi.org/10.1117/12.578196

[26] Fechteler, P., Eisert, P., & Rurainsky, J. (2007, September). Fast and high resolution 3D face scanning. *In 2007 IEEE International Conference on Image Processing* (Vol. 3, pp. III–81). IEEE. https://doi.org/10.1109/ICIP.2007.4379251

[27] Structured-light 3D scanner (2021, June 5). In *Wikipedia*. https://en.wikipedia.org/wiki/Structured-light_3D_scanner

[28] Erf, R. K. (1978). *Speckle metrology*. Academic Press.

[29] OPTEC. (2021). *Optical fibre image guides* [Brochure].

[30] Igielski, J., Kujawinska, M., & Pawlowski, Z. (1995, May). Automatic photolaryngoscope for vibration analysis of vocal cords. *In Lasers in Surgery: Advanced Characterization, Therapeutics, and Systems V* (Vol. 2395, pp. 360–364). SPIE. https://doi.org/10.1117/12.209098

[31] Wojtaszewski, A., Kujawińska, M., Igielski, J., & Rafałowski, M., (1994). Sposób rejestracji drgań strun głosowych (Patent RP 175300). (in Polish)

[32] Wegiel, M., & Kujawinska, M. (2006). Fast 3D shape measurement system based on colour structure light projection. In *Fringe 2005* (pp. 450–453). Springer, Berlin, Heidelberg. https://doi.org/10.1007/3-540-29303-5_60

[33] Van der Jeught, S., & Dirckx, J. J. (2017). Real-time structured light-based otoscopy for quantitative measurement of eardrum deformation. *Journal of Biomedical Optics*, *22*(1), 016008. https://doi.org/10.1117/1.JBO.22.1.016008

[34] Szymański, M., Rusinek, R., Zadrożniak, M., Warmiński, J., & Morshed, K. (2009). Drgania błony bębenkowej oceniane Dopplerowskim wibrometrem laserowym. *Otolaryngologia Polska*, *63*(2), 182–185. https://doi.org/10.1016/S0030-6657(09)70103-9

[35] Podbielska, H. (1991). Endoscopic profilometry. *Optical Engineering*, *30*(12), 1981–1985. https://doi.org/10.1117/12.56009

[36] Kasprzak, H. T., & Podbielska, H. (1994, February). Speckle photography in biomechanical testing. *In Microscopy, Holography, and Interferometry in Biomedicine* (Vol. 2083, pp. 268–279). SPIE. https://doi.org/10.1117/12.167444

[37] Belovolov, M. I., Paramonov, V. M., Belovolov, M. M., Svistushkin, M. V., Svistuskin, V. M., Arkhipov, M. V., Mokoyan, Z. T., Timofeeva, V. A., Kotova, S. L., Timashev, P. S. & Timashev, S. F. (2020). Vibration activity of the vocal folds and a new instrumental technique for their study. *Optical Engineering*, *59*(6), 061611. https://doi.org/10.1117/1.OE.59.6.061611

[38] Silva, J. N., Southworth, M., Raptis, C., & Silva, J. (2018). Emerging applications of virtual reality in cardiovascular medicine. *JACC: Basic to Translational Science*, *3*(3), 420–430. https://doi.org/10.1016/j.jacbts.2017.11.009

[39] Duan, Y. Y., Zhang, J. Y., Xie, M., Feng, X. B., Xu, S., & Ye, Z. W. (2019). Application of virtual reality technology in disaster medicine. *Current Medical Science*, *39*(5), 690–694. https://doi.org/10.1007/s11596-019-2093-4

[40] Samadbeik, M., Yaaghobi, D., Bastani, P., Abhari, S., Rezaee, R., & Garavand, A. (2018). The applications of virtual reality technology in medical groups teaching. *Journal of Advances in Medical Education & Professionalism*, *6*(3), 123. https://doi.org/10.30476/JAMP.2018.41023

Andrzej Zając received the M.Sc. degree in technical physics in 1979, the Ph.D. degree in electronics in 1987, both from the Military University of Technology in Warsaw and habilitation in electronics in 1998 from the Military University of Technology in Warsaw. From 1979 to 2021 he worked at the Institute of Optoelectronics Military University of Technology in Warsaw, where he was engaged in the investigations of laser systems and optical measuring methods for medical application. Since 2001 he has been a professor at the Military University of Technology. Author of more than 300 scientific publications.

Szymon Nitkiewicz obtained Master's degree in Mathematics in 2006, then graduated a PhD in Biocybernetics and Biomedical Engineering in 2018. His experience in mathematics allows him to analyze in detail a wide range of issues. His scientific interests oscillate in topics related to supporting medical diagnostics, as well as in assessing the impact of human activity on the environment. He is an author and co-author of more than 20 research papers with summary He is an owner of few Patents for devices that were awarded at International exhibitions.

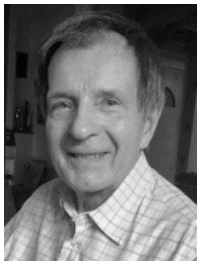

Andrzej Kukwa started medical studies in 1959at the Medical University of Warsaw. He defended his PhD in 1971 and obtained his habilitation in medical science, in 1974. The position of full professor at the Medical Academy, Warsaw in 1990. A head Otolaryngology Clinic, Department of Dentistry, Medical Academy of Warsaw from 1989 to October 2011. And then from October 1 I was employed as the head of the Department and Clinic of Otorhinolarygology of Head and Neck Surgery at the University of Warmia and Mazury in Olsztyn. He has received a scholarship four times in the USA. He is the author or co-author of over 200 papers, and the co-author of several patent solutions. He is promotor of 11 doctoral dissertations, tutor of 20 specialization for the 1st and 2nd degree in Otolaryngology.

Edyta Zomkowska, completed her specialization in clinical speech and language pathology in 2015 at the Department of Phoniatrics and Audiology of the Heliodor Święcicki Clinical Hospital at the Poznań University of Medical Sciences. In 2017, she obtained an PhD degree from the Faculty of Medicine at the University of Warmia and Mazury in Olsztyn. Since 2011 she works at the Department of Otorhinolaryngology, Head and Neck Surgery and the Clinical Department of Neurological and Systemic Rehabilitation of the University Clinical Hospital in Olsztyn. The focus of her professional work is issues related to swallowing disorders and breathing difficulties during sleep.

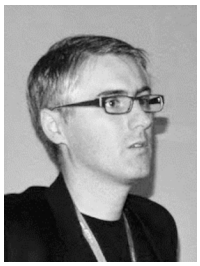

Robert Barański received the M.Sc. degree in mechanical engineering in 2002, the Ph.D. degree in mechanics in the field of vibroacoustics, in 2007, and the DSc. degree in mechanics in the field of engineering and technical sciences in 2019. Since 2006, he has been working at Department of Mechanics and Vibroacoustics, AGH-University. His scientific interests focus on biomechanics, EMG signals analysis, embedded system, diagnostic and measurement systems.

Adam Rybak was born in Ciechanów, Poland, in 1989. He received the B.Eng. (2013) degree from Warsaw University of Technology (WUT), Poland and an M.Sc. degree in electronic engineering and telecommunications in 2016 in Optoelectronics Institute from the Military University of Technology (MUT) in Warsaw, Poland. He is currently pursuing the Ph.D. degree in the Military University of Technology (MUT) in Warsaw, Poland. His research activity is focused on the application of optoelectronics in medicine.